



UNIVERSITY OF LEEDS

This is a repository copy of *Mesophase pitch-based graphite fiber-reinforced acrylonitrile butadiene styrene resin composites with high thermal conductivity*.

White Rose Research Online URL for this paper:
<http://eprints.whiterose.ac.uk/91960/>

Version: Accepted Version

Article:

Yuan, G, Li, X, Yi, J et al. (7 more authors) (2015) Mesophase pitch-based graphite fiber-reinforced acrylonitrile butadiene styrene resin composites with high thermal conductivity. *Carbon*, 95. 1007 - 1019. ISSN 0008-6223

<https://doi.org/10.1016/j.carbon.2015.09.019>

© 2015. This manuscript version is made available under the CC-BY-NC-ND 4.0 license
<http://creativecommons.org/licenses/by-nc-nd/4.0/>

Reuse

Unless indicated otherwise, fulltext items are protected by copyright with all rights reserved. The copyright exception in section 29 of the Copyright, Designs and Patents Act 1988 allows the making of a single copy solely for the purpose of non-commercial research or private study within the limits of fair dealing. The publisher or other rights-holder may allow further reproduction and re-use of this version - refer to the White Rose Research Online record for this item. Where records identify the publisher as the copyright holder, users can verify any specific terms of use on the publisher's website.

Takedown

If you consider content in White Rose Research Online to be in breach of UK law, please notify us by emailing eprints@whiterose.ac.uk including the URL of the record and the reason for the withdrawal request.



eprints@whiterose.ac.uk
<https://eprints.whiterose.ac.uk/>

Mesophase pitch-based graphite fiber-reinforced acrylonitrile butadiene styrene resin composites with high thermal conductivity

Guanming Yuan ^{a, b}, Xuanke Li * ^{a, b}, Jing Yi ^b, Zhijun Dong ^{a, b},
Aidan Westwood ^c, Baoliu Li ^b, Zhengwei Cui ^b, Ye Cong ^b, Jiang Zhang ^b, Yanjun Li ^b

a The State Key Laboratory of Refractories and Metallurgy, Wuhan University of Science and Technology, Wuhan 430081, China;

b Hubei Province Key Laboratory of Coal Conversion & New Carbon Materials, Wuhan University of Science and Technology, Wuhan 430081, China;

c Institute for Materials Research, University of Leeds, Leeds LS2 9JT, United Kingdom.

Abstract: One-dimensional (1-D) and two-dimensional (2-D) mesophase pitch-based graphite fiber (MPGF) / acrylonitrile butadiene styrene (ABS) resin composites were prepared from unidirectionally arranged MPGF/ABS resin laminae by a hot-press method. The morphologies, optical texture and crystal structure of the MPGFs and their ABS resin composites were investigated. The influence of the volume fraction, diameter and graphitization temperature of the MPGFs and the composite architecture on the thermal properties of the composites was discussed. The thermal diffusivity and thermal conductivity of the resultant composites parallel to the longitudinal fiber direction increase markedly with the volume fraction, diameter and graphitization temperature of the fibers. The 1-D composite with a fiber volume fraction of 62% possesses a bulk density of 1.64 g/cm³ and shows a high thermal diffusivity of 372

* Corresponding author. Tel.: Fax: +0086 27 86556906
E-mail address: xkli8524@sina.com (X. Li)

mm²/s and a high thermal conductivity of 518 W/m K parallel to the longitudinal fiber direction at room temperature. The corresponding axial thermal conductivity of the fibers, graphitized at 2900 °C with a diameter of 50~55 μm, is estimated to be 825 W/m K. The 2-D composite filled with a high (54%) volume fraction of MPGFs also exhibits a high thermal conductivity in two directions (parallel to the longitudinal directions of the incorporated fibers).

1. Introduction

Heat generated by electronic devices and circuitry must be dissipated to improve performance, reliability and prevent premature failure [1]. Currently, utilization of high-conductivity materials is proposed to solve thermal management problems (heat dissipation, thermal stress and warping) in microelectronics, high-power devices and their assemblies or packaging [2-4]. Pitch-based carbon fibers are unique in their ability to achieve ultra-high Young's modulus and thermal conductivity and, therefore, have found an assured place in thermal management applications [5-7]. Recently, the application range of pitch-based carbon fiber-reinforced carbon matrix (C/C) composites with high thermal conductivity, has been broadened from critical military and aerospace applications to include thermal management (heat sinks) in electronic components and heat pipes [8-10]. However, the thermal conductivity of C/C composites is structure sensitive (directionally dependent). The composite architecture, thermal conductive property, filler volume fractions, crystal orientation and crystallinity of carbon fiber fillers themselves, as well as the spatial arrangement of voids and other defects in C/C composites, have obvious influence on their thermal conductivity. In consequence, the preparation process for such highly conductive C/C composites is extremely complicated, coupled with a long fabrication period and high

production cost, which has greatly hindered their widespread commercialization [11,12]. In addition, all C/C composites share a common disadvantage of being electrically conductive, which is undesirable in many microelectronic applications.

Instead, carbon fiber-reinforced polymer matrix composites, which also offer good thermal performance, have been shown to overcome these disadvantages. They can be simply fabricated at a relatively low cost and easily machined into finished products, and thus are extensively used in thermal management fields [1-4,13]. For instance, vapor grown carbon fiber-reinforced epoxy matrix composite hot-pressed at 150 °C exhibits a thermal conductivity as high as 695 W/m K in the direction parallel to the oriented fibers with a density of 1.5 g/cm³, and it has an electrically insulating surface unlike carbon fiber-reinforced carbon or metal matrix composites [14]. The preparation of semi-aligned and semi-continuously aligned vapor grown carbon fibers with ultrahigh axial thermal conductivity is a key factor for these high thermal conductivity composites. However, such composites are not easily manufactured with large size due to the discontinuities and misalignments of vapor grown carbon fibers (commonly limited in length and entangled together) when used as fillers in composites. On the other hand, as continuous and controllable fibers with high axial thermal conductivity, mesophase pitch-based carbon fibers have found applications as thermal management materials [1-4] due to their excellent thermal transport properties. The commercial carbon fiber with the highest thermal conductivity at present is K-1100, manufactured by BP-Amoco Performance Products, which has a renowned axial thermal conductivity of 1100 W/m K. It is important to note that a continuous K-1100 carbon fiber-reinforced epoxy matrix composite with a fiber volume fraction of 60% having all fibers oriented in the same direction, would have an extraordinary axial thermal conductivity of 540~660 W/m K, which is almost 1.5 times that of

copper (about 400 W/m K) [2,3,15]. Compared with continuous ones, discontinuous (chopped or milled) K-1100 carbon fiber-reinforced polymer matrix composites, in contrast, show an approximately isotropic thermal conductivity of below 20 W/m K. Thus, a major advantage of using continuous carbon fibers is that it is possible to translate their excellent properties into composites and to vary directional properties significantly. For example, by orienting a high percentage of continuous fibers, it is feasible to produce composites with very high thermal conductivities along the carbon fiber axis. This can make fiber-reinforced composites more efficient than heat pipes in transporting heat over relatively short distances in some instances. An additional benefit is that solid-state methods of heat transfer are more reliable [3]. In addition to their high thermal conductivity, mesophase pitch-based carbon fibers have other attractive attributes for packaging applications, such as extremely high modulus (stiffness) – e.g. K-1100 fiber's elastic modulus is as high as 965 GPa, more than an order of magnitude greater than that of aluminum (69 GPa) – relatively low density (2.2 g/cm³) to save weight and low, or even negative ($-1.5 \times 10^{-6} \text{ } ^\circ\text{C}^{-1}$) axial coefficient of thermal expansion to more closely match other relatively low thermal expansions (e.g. that of silicon) throughout the system, etc. [3].

This work reports the preparation and characterization of continuous mesophase pitch-based graphite fiber (MPGF) reinforced acrylonitrile butadiene styrene (ABS) resin composites. The objective of this work is to show the influence of the carbon fibers' volume fraction, diameter and graphitization temperature on the thermal diffusivity and thermal conductivity of composites filled with carbon fibers in one direction, or in two orthogonal directions. The electrical resistivity and mechanical properties of the resultant one-dimensional (1-D) and two-dimensional (2-D) ABS resin composites are also reported. Furthermore, the room-temperature axial thermal

conductivity of MPGFs is estimated reasonably and accurately by measuring the thermal diffusivity and thermal conductivity of the 1-D composites.

2. Experimental

2.1 Raw materials

Round-shaped MPGFs were prepared by melt-spinning a commercial naphthalene-derived synthetic mesophase pitch (produced by Mitsubishi Gas Chemical Corporation) followed by complete oxidative stabilization, carbonization and final graphitization at 2500, 2700 and 2900 °C [16]. These MPGFs had various diameters in the range of 10~55 μm (and each batch typically has a slight, $\pm 5 \mu\text{m}$, differential in diameter owing to multi-hole spinning).

ABS resin was purchased from Zhenjiang Chimei Plastic Company in Jiangsu province of China. The typical composition of ABS resin is approximately 25% acrylonitrile, 25% butadiene, and 50% styrene by weight. The softening point and density of ABS resin are about 100 °C and 1.05 g/cm^3 , respectively.

2.2 Preparation of the MPGF/ABS resin composites

ABS resin particles weighed at a required percentage to carbon fiber were directly dissolved in acetone by magnetic stirring for 5 h to form a homogeneous solution. The weighed MPGF bundles (aligned well during the whole preparation process) were arranged at a low thickness of about 0.3 mm in a rectangular-shaped plastic mould. The ABS resin solution was carefully cast on the ordered MPGF array, and the MPGFs were uniformly soaked with the solution. A lamina of MPGF/ABS resin prepreg is formed after complete volatilization of the acetone in a draught cupboard. Many laminas with a size of 80 \times 40 mm were mechanically cut from these thin prepreps and then piled up uniaxially in a stainless steel mould, and finally

hot-pressed at 180 °C for 2.5 h under a pressure of 1 MPa to produce a unidirectional laminate with a dimension of 80 × 40 × 10 mm, namely a 1-D MPGF/ABS resin composite block. Orthogonally arranged laminas were also stacked alternately in the mould, and 2-D MPGF/ABS resin composite blocks loaded with different fractions of MPGFs were prepared by an identical hot-pressing procedure. The fiber volume fraction (V_f) in the composites was approximately determined by measuring the specific gravities of the composites (d_c), matrix resin (d_m) and graphite fibers (d_f) using the equation: $V_f = (d_c - d_m) / (d_f - d_m)$ [17].

2.3 Characterization of the MPGF/ABS resin composites

Test specimens were mechanically cut from the as-prepared MPGF/ABS resin composite blocks, polished with abrasive paper and ultrasonically washed in ethanol for 0.5 h. The crystalline parameters of MPGFs and the structural preferred orientation of the resultant composite blocks were determined by X-ray diffraction (XRD) analysis using Cu K_α radiation ($\lambda = 0.15406$ nm). The microstructure, morphology and optical texture of the MPGFs and their ABS resin composites were imaged with a TESCAN VEGA3 scanning electron microscope (SEM) and a Carl Zeiss AX10 polarized light microscope (PLM) in reflectance mode.

The room-temperature electrical resistivity of the prepared rectangular-shaped composite block was directly measured by the standard four-probe method on a TTI BS 407 precision milli/micro ohmmeter. The bulk density (ρ) of the composite block with a regular shape was calculated from its mass and dimensions. The thermal diffusivity (α) of a composite specimen with a size of 10 × 10 × 4 mm was measured using a laser-flash diffusivity instrument (LFA 447, NETZSCH) at room temperature. Each sample was tested in at least three sections and the average thermal diffusivity of the three measurements was calculated. Both the electrical resistivity and thermal

diffusivity data were primarily obtained along the longitudinal direction of graphite fibers. It is well known that specific heat capacity (C_p) is a material constant and is sensitive to the ambient temperature. The values of C_p of the MPGF/ABS resin composites were not easy to determine precisely by using a differential scanning calorimeter at room temperature (25 °C). Consequently, the C_p values of the composites were estimated from those of the two components, ABS resin and MPGF, according to the mixture rule [18,19]. The room-temperature C_p values of ABS resin and the 2900 °C graphitized MPGFs are reported respectively as 1.30 and 0.71 J/g K [18,19], and the room-temperature C_p values of the composites could thus be calculated, changing (like density) relatively little from 1.14 to 0.85 J/g K as the fiber volume fractions varied markedly from 15% to 62%. Therefore, the thermal diffusivity value was determined to be the most critical factor governing the thermal conductivity of the composite materials. The thermal conductivity (λ) of the composites was calculated from the bulk density, specific heat capacity and thermal diffusivity according to the equation: $\lambda = \rho \cdot C_p \cdot \alpha$. The impact strengths of MPGF/ABS resin composite blocks were measured on normal bar specimens (about 80 × 10 × 4 mm) perpendicular to the longitudinal direction of graphite fibers at room temperature using a ZWJ-0350 simple beam impact testing machine.

3. Results and discussion

3.1 Morphology and structure of the MPGFs

Fig. 1(a) shows a typical optical photograph of the as-spun round-shaped pitch fibers. It can be seen from Fig. 1(a) that the pitch fibers are well aligned on a flat metal plate. Such aligned pitch fibers were carefully transferred onto a flexible graphite plate for in-situ oxidative stabilization, carbonization and graphitization

treatments, in order to obtain ordered MPGFs for preparing the directional composites. The PLM photograph shown in Fig. 1(b) exhibits the transverse section of large diameter carbon fibers graphitized at 2500 °C, which shows a typical “Pac-man” open crack texture. Fig. 1(c-f) shows the typical SEM images of round-shaped MPGFs with different diameters in the range of 10~55 μm. It is clear that almost all large MPGFs with a diameter of 50~55 μm as shown in Fig. 1(c) present an obvious radial crack morphology and the angle of the open wedge crack seems to be above 90°. With the decrease of MPGF diameter, the degree of splitting and the abundance of cracks in the fibers are significantly reduced. In particular, no obvious cracks can be observed in the transverse sections of the MPGFs with a diameter of 10~15 μm as shown in Fig. 1(f). The open wedge-shaped splitting texture shown in Fig. 1(c-e) may be caused by internal stresses within such highly oriented fibrous materials, caused by anisotropic shrinkage during preferential orientation of crystallites in the fibers (as shown in Fig. 2a) during graphitization treatment. However, the splitting of the fibers enables the graphene layers to pack and register more perfectly, which results in a higher modulus and conductivity in the fiber axial direction [20]. The benchmark graphite fibers (K-1100) with very high axial thermal conductivity also similarly form an open wedge crack structure at the transverse section [16,21]. Although such cracks can be reduced or eliminated by precise control of spinning parameters [22,23], the round-shaped carbon fibers exhibiting radial texture in their transverse cross sections remain prone to splitting during high-temperature heat treatment.

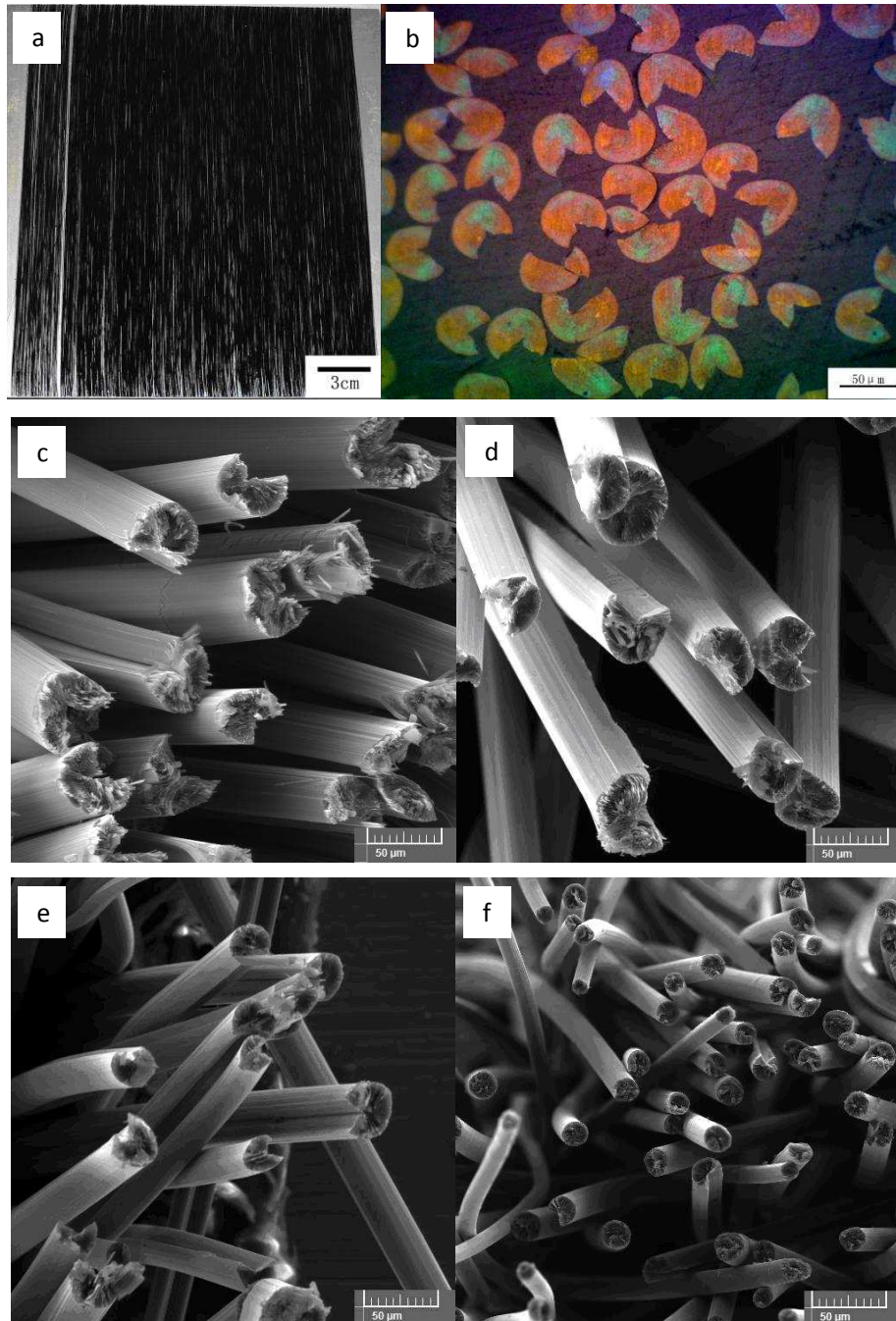


Fig. 1 (a) Optical photograph of well-aligned pitch fibers on a flat plate, (b) typical PLM micrograph and (c-f) SEM images of 2500 °C graphitized MPGFs with various diameters (b, c-50~55, d-28~32, e-18~22, f-10~15 μm).

As shown in Fig. 2(a), the carbon layers of a radial-textured MPGF with a large diameter of $\sim 55 \mu\text{m}$ after graphitization at 2900 °C are obviously developed from the surface to the centre of the fiber, which is similar to the transverse textural diagram of

a graphite fiber shown in Fig. 2(b). The highly preferred orientation of carbon layers running along the axial direction of fiber is clearly observed in Fig. 1(c) and Fig. 2(a).

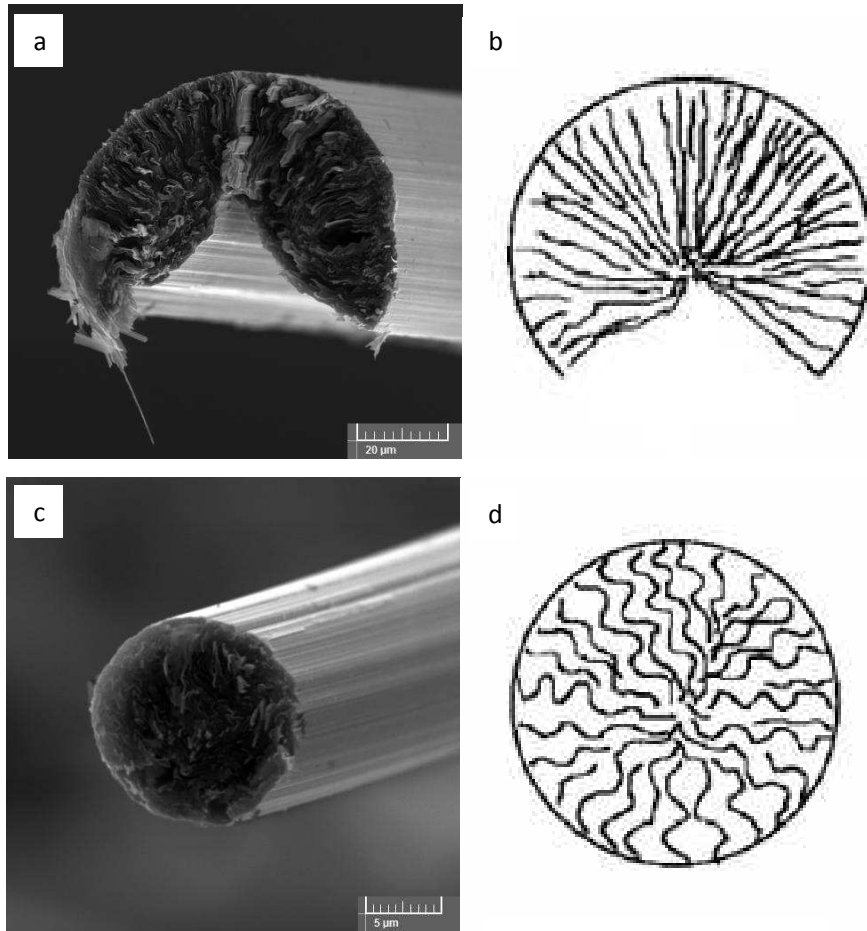


Fig. 2 Typical SEM images of a single round-shaped carbon fiber with (a) large and (c) small diameters graphitized at 2900 °C and its corresponding transversal textural diagram (b and d).

In contrast, the graphite fiber with a small diameter of $\sim 10 \mu\text{m}$ exhibits a radial-folded or disturbed texture in the transverse section of fiber as shown in Fig. 2(c), and the microcrystal domains or carbon layers are bent, twisted or waved as sketched in Fig. 2(d), which may be disadvantageous to the growth of microcrystal graphite and also effectively prohibits the propagating of cracks so as to preserve morphological

integrity. This suggests that the preferred orientation and microcrystal domains of graphite crystals in the larger diameter fiber are greater than those in a small one [24]. The XRD analyses shown in Fig. 3 further verify this conjecture. The relative intensity of the (0 0 2) diffraction peak of large diameter fibers is much stronger than that of small diameter fibers. The former indicates more perfect orientation of carbon layers and the larger crystal size, which is highly consistent with the SEM observation results.

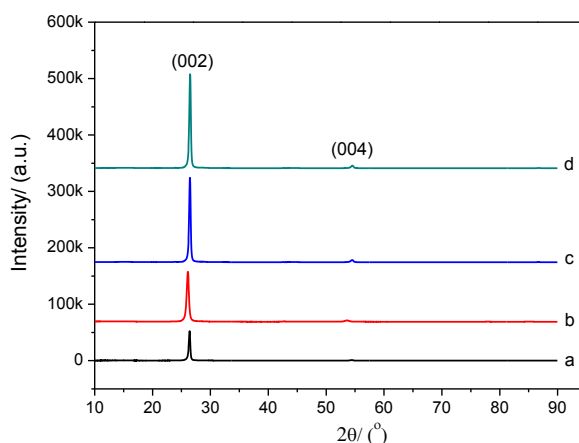


Fig. 3 XRD patterns of the 2500 °C graphitized MPGFs with different diameters (a-10~15, b-18~22, c-28~32, d-50~55 μm).

Being calculated from the XRD patterns after correction for instrument broadening using Si as an internal standard, the crystal coherence length ($L_{a(002)}$) [25], the stacking height ($L_{c(002)}$) and the degree of graphitization (g) [26] of the MPGFs with different diameters are listed in Table 1. Although the interlayer spacing (d_{002}) values of the MPGFs do not decrease much with increasing fiber diameter, the crystalline parameters ($L_{c(002)}$ and $L_{a(002)}$ values) and g values of the MPGFs are obviously increased with the increase of fiber diameter and graphitization temperature. The plane orientation of graphite crystals also increases with heat treatment temperatures.

Such larger diameter MPGFs with a radial transverse texture exhibiting bigger crystalline sizes, higher g values and better crystalline orientation, can undoubtedly offer a high thermal conductivity similar to K-1100 fibers [24,27].

Table 1 Crystalline parameters and graphitization degree of the 2500 and 2900 °C graphitized MPGFs with various diameters.

$\Phi/\mu\text{m}$	$2\theta_{002}/^\circ$	d_{002}/nm	$L_{C(002)}/\text{nm}$	$L_{a(002)}/\text{nm}^a$	$g/\%^b$
10~15	26.38	0.3375	24.11	45.24	75.6
18~22	26.39	0.3374	24.25	47.50	76.7
28~32	26.40	0.3373	24.88	50.00	77.9
50~55	26.41	0.3372	26.72	52.78	79.1
10~15 ^c	26.42	0.3371	28.41	55.88	80.2
50~55 ^c	26.45	0.3367	30.29	73.08	84.8

a $L_{a(002)}$ values were calculated by the relation $L_a = 9.5 / (d_{002} - 3.354)$ [25].

b Degree of graphitization (g) was calculated by the expression $g = (0.3440 - d_{002}) / (0.3440 - 0.3354)$ [26].

c 2900 °C graphitization treatment.

3.2 XRD characterization of the MPGF/ABS resin composites

Fig. 4 shows the orientation and arrangement diagrams of carbon fibers in 1-D and 2-D MPGF/ABS resin composites produced by a hot-press method. The hot-pressed surface and transverse section of the composite blocks are labeled in the figures.

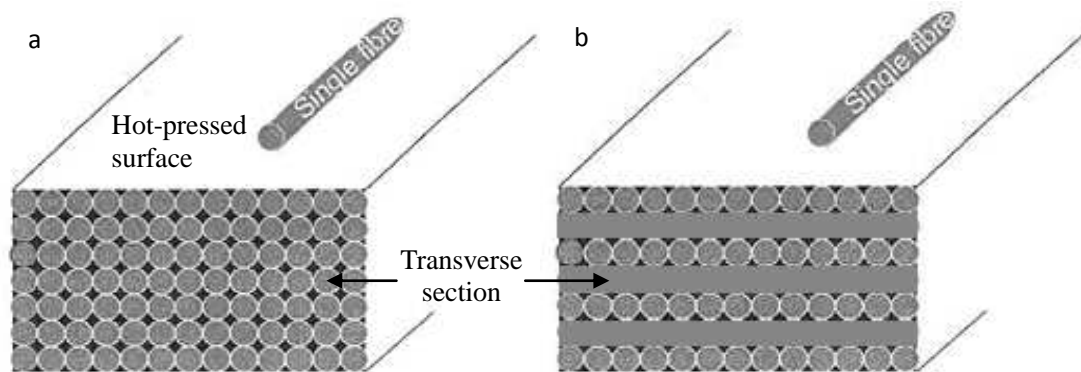


Fig. 4 The orientation and arrangement of carbon fibers in (a) 1-D and (b) 2-D MPGF/ABS resin composites.

Typical XRD patterns, from the hot-pressed surface shown in Fig. 5(a) and the transverse section shown in Fig. 5(b), were obtained for the 1-D MPGF/ABS resin composites made with 2500 °C graphitized fibers of various diameters at a fixed volume fraction of 36%. There is one intense peak at about $2\theta = 26.4^\circ$ and another weak peak at roughly $2\theta = 54.6^\circ$ in Fig. 5(a), which can be attributed to (0 0 2) and (0 0 4) crystal planes of hexagonal graphite fibers, and no other peaks are observed due to the highly oriented carbon layers in the graphite fibers [28]. The relative intensity of the (0 0 2) diffraction peak of the composites obviously increases with the diameter of fibers, which is in good agreement with the XRD profiles of carbon fibers shown in Fig. 3. In comparison with the XRD profiles shown in Fig. 5(a), Fig. 5(b) shows a weak and broad amorphous diffraction peak at $2\theta = 20.2^\circ$ attributed to the ABS resin and two sharp diffraction peaks at about $2\theta = 42.4$ and 77.5° corresponding to the (1 0 0) and (1 1 0) crystal planes of hexagonal graphite. It is interesting to note that the strong (0 0 2) diffraction peak in Fig. 5(a) disappears completely in Fig. 5(b). The XRD profiles in Fig. 5(a and b) show that the crystal orientation of the sample is highly anisotropic, which is the result of the ordered arrangement of the highly oriented graphite fibers in the composite. This indicates that all MPGFs are uniformly

aligned in the direction perpendicular to the transverse section of the composite block [29,30], which is highly consistent with the diagram of the idealized 1-D composite block shown in Fig. 4(a) above. The significant orientation of carbon fibers in the composite may lead to anisotropic thermal conductivity in the composite, due to the continuity and discontinuity, respectively, of carbon fibers within the hot-pressed surface and transverse section of the 1-D MPGF/ABS resin composites.

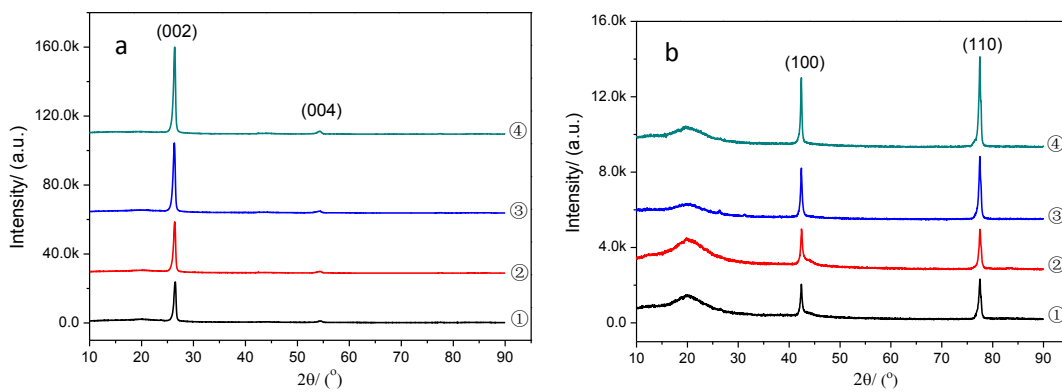


Fig. 5 XRD patterns of (a) hot-pressed surface and (b) transverse section of the 1-D MPGF/ABS resin composites made with fibers of various diameters at a fixed volume fraction of 36% (①-10~15, ②-18~22, ③-28~32, ④-50~55 μm).

The XRD patterns of the hot-pressed surface and the transverse section of the 1-D MPGF/ABS resin composites made with different volume fractions of 2500 °C graphitized fibers with a fixed diameter of 50~55 μm are shown in Fig. 6(a and b). These XRD patterns show a varying trend similar to that in Fig. 5(a and b), indicating that the composite blocks also possess oriented structure due to the 1-D ordered arrangement of MPGFs in ABS resin. The relative intensity of the (0 0 2) diffraction peak of the hot-pressed surface in Fig. 6(a) is generally stronger than that of the composites as shown in Fig. 5(a), as a result of the larger crystal size and higher

volume fraction of large-diameter MPGFs.

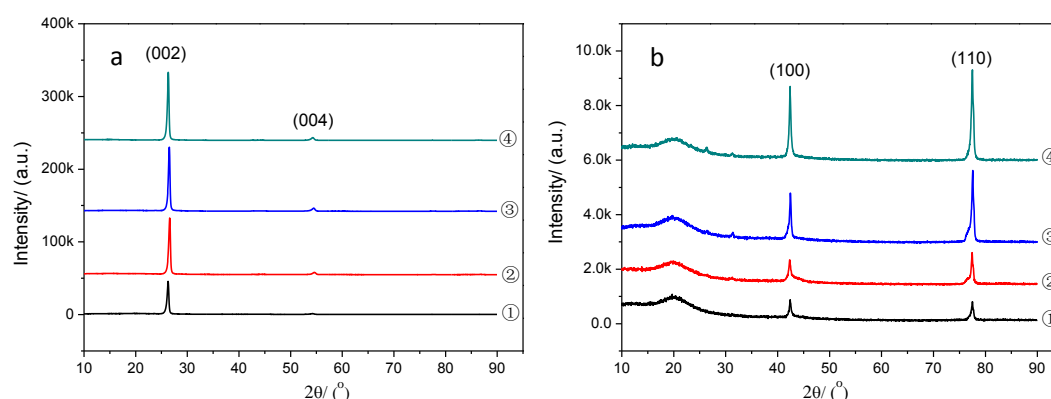


Fig. 6 XRD patterns of (a) hot-pressed surface and (b) transverse section of the 1-D MPGF/ABS resin composites with varying volume fractions of fibers of diameter 50~55 μm (①-25%, ②-36%, ③-45%, ④-54%).

The hot-pressed surface of the 2-D MPGF/ABS resin composite block made with various volume fractions of 2500 °C graphitized fibers of various diameters shows similar XRD profiles (not shown) to those of the 1-D MPGF/ABS resin composite as shown in Fig. 5(a) and Fig. 6(a). The XRD profiles in Fig. 7(a and b) are from the transverse sections of the 2-D MPGF/ABS resin composite blocks made with fibers of various diameters and various volume fractions of fibers, respectively. One intense diffraction peak at about $2\theta = 26.4^\circ$ and three other weak diffraction peaks at around $2\theta = 42.4, 54.6$ and 77.5° attributed to (0 0 2), (1 0 0), (0 0 4) and (1 1 0) crystal planes of hexagonal graphite can be observed in Fig. 7(a and b). Owing to the differing arrangement architectures (1-D or 2-D) of the MPGFs in the composites, the relative intensities of diffraction peaks from the transverse section in Fig. 7(a and b) are obviously stronger ((0 0 2)) and weaker ((1 0 0) and (1 1 0)) than those of the composites shown in Fig. 5(b) and Fig. 6(b). It is well known that the XRD equatorial

and meridional scans for MPGFs show a significant difference due to their highly anisotropic structure [16].

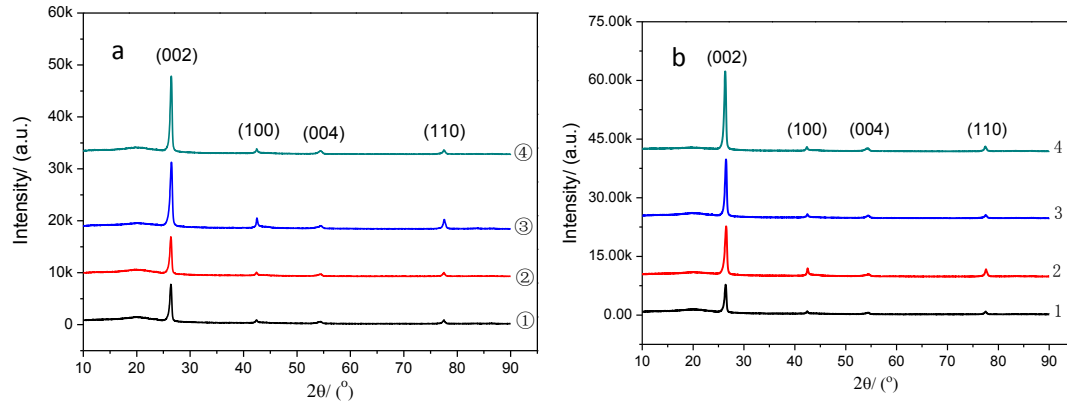


Fig. 7 XRD patterns of the transverse section of the 2-D MPGF/ABS resin composites varying with (a) the diameters of fibers at a fixed volume fraction of 36 vol.% (①-10~15, ②-18~22, ③-28~32, ④-50~55 μm) and (b) the volume fractions of fibers with a diameter of 50~55 μm (1-25%, 2-36%, 3-45%, 4-54%).

Fig. 8 shows typical XRD patterns of the hot-pressed surface and transverse section of the 1-D and 2-D MPGF/ABS resin composites made with 50~55 μm fibers graphitized at various temperatures at a fixed volume fraction of 36%. It can be clearly seen that the relative intensities of (0 0 2) and (1 0 0) or (1 1 0) diffraction peaks of the composites obviously increase with the graphitization temperature, which indicates that the MPGFs treated at a higher graphitization temperature possess more perfect orientation of carbon layers and a larger crystal size [12,16]. This may lead to the better thermal conduction property of the resultant MPGF/ABS resin composites. The relative intensity of the (0 0 2) diffraction peak of the hot-pressed surface of the 2-D composites is roughly twice that of the transverse section, which is the result of the alternating arrangement of the MPGFs at 0 and 90°.

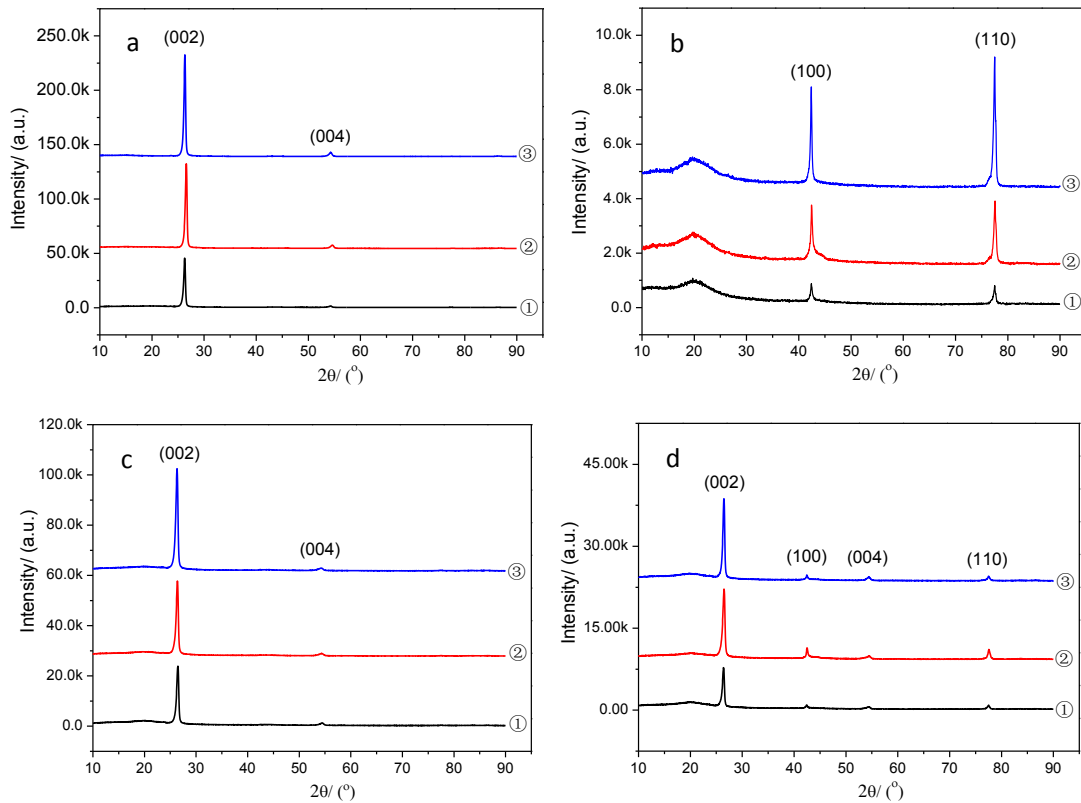


Fig. 8 XRD patterns of (a and c) hot-pressed surface and (b and d) transverse section of the 1-D (a and b) and 2-D (c and d) MPGF/ABS resin composites made with 50~55 μm fibers at a fixed volume fraction of 36% graphitized at various temperatures (①-2500, ②-2700, ③-2900 $^{\circ}\text{C}$).

3.3 PLM and SEM observation of the MPGF/ABS resin composites

Typical PLM and SEM images from the transverse section and the longitudinal section (parallel to the longitudinal direction of fibers and perpendicular to the transverse section) of the 1-D MPGF/ABS resin composite block made with 2500 $^{\circ}\text{C}$ graphitized fibers with a diameter of 50~55 μm at a volume fraction of 54% are shown in Fig. 9. These typical images clearly indicate the parallel, unidirectional arrangement of the MPGFs in the composite, which corresponds well with the diagram of the 1-D composite block shown in Fig. 4(a) and is consistent with the

absence of the (0 0 2) diffraction peak from XRD patterns obtained from the transverse section of the 1-D composite blocks as shown in Fig. 5(b) and Fig. 6(b). The MPGFs still maintain their open wedge-shaped splitting morphology and seem to be uniformly distributed in the composites. There is no debond or crack occurring at the interface between the MPGFs and ABS resin except for slight scratches caused by the polishing treatment. The orderly arrangement of continuous MPGFs parallel to each other in the composite block can be expected to aid thermal transport along the longitudinal direction of fibers, as will be shown subsequently.

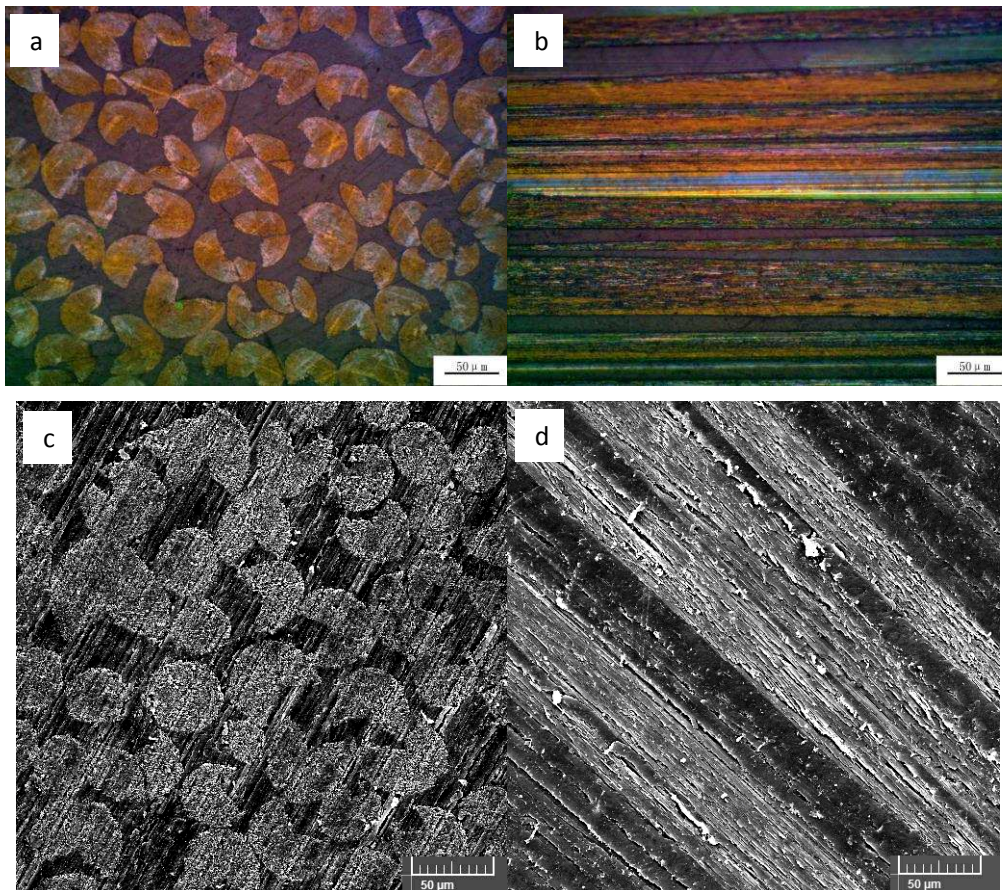


Fig. 9 Typical (a and b) PLM photographs and (c and d) SEM images of transverse (a and c) and longitudinal (b and d) sections of the 1-D MPGF/ABS resin composites made with 54 vol.% MPGFs with a diameter of 50~55 μm .

Fig. 10 shows typical low-magnification PLM and SEM images of transverse sections of the 2-D MPGF/ABS resin composite made with 54 vol.% MPGFs with a diameter of 50~55 μm . The ordered orthogonal arrangement of the carbon fibers can be clearly observed in these transverse sections.

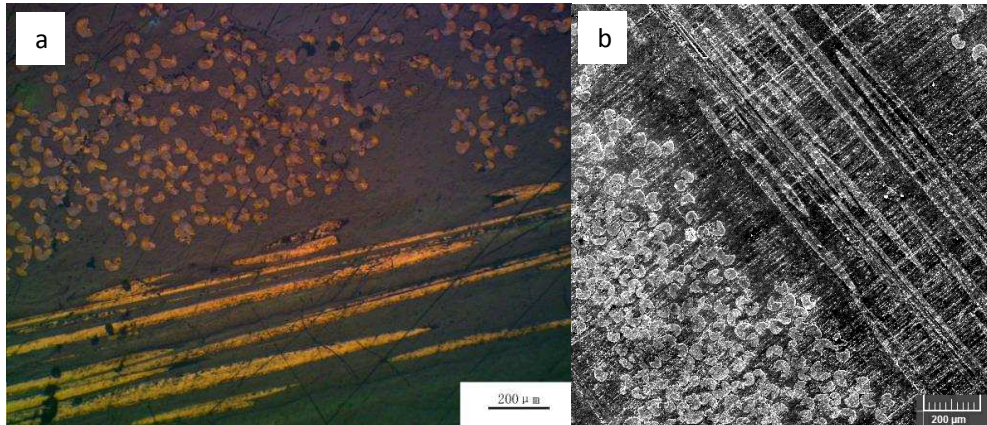


Fig. 10 Typical (a) PLM photograph and (b) SEM image of transverse sections of the 2-D MPGF/ABS resin composite made with 54 vol.% MPGFs with a diameter of 50~55 μm .

3.4 Thermal properties of the MPGF/ABS resin composites

Fig. 11 shows that the room-temperature thermal diffusivities of the 1-D MPGF/ABS resin composites along the fiber longitudinal direction increase markedly with the volume fractions, diameters and graphitization temperatures of the fibers. The 1-D composites made with larger diameter fibers clearly exhibit higher thermal diffusivity values. There are obvious differences between the thermal diffusivities of composites made with MPGFs of diameters above 30 μm and those below 20 μm , which are closely associated with the transverse microstructure and crystal orientation of the MPGFs as shown in Fig. 1 and Fig. 2. As listed in Table 1, the crystallite size and graphitization degree of MPGFs increase with the diameter of MPGFs, which

significantly increases the thermal conductivity of their composites. With the increase of graphitization temperature from 2500 to 2900 °C, the significant increase of the thermal diffusivities of the composites made with the same volume fraction of fibers can be attributed to the more perfect orientation of carbon layers and the larger crystal size within MPGFs heat-treated at higher temperature. The ABS resin matrix possesses a very low thermal diffusivity of 0.14 mm²/s, which contributes little to the thermal conduction of the composites. When the volume fraction of MPGFs increases to 62%, the 1-D composite block made with the 2900 °C graphitized fibers having a large diameter of 50~55 μm possesses a high thermal diffusivity of 372 mm²/s. As a comparison, the thermal diffusivity value for copper is only ~117 mm²/s [31].

The thermal diffusivities of 1-D composite blocks made with the 2900 °C graphitized fibers with diameters of 50~55 and 10~15 μm as they vary with the fiber volume fractions in the range from 15% to 62% are presented with their curve fits in Fig. 11(d). As can be seen from the curve in Fig. 11(d), there is a reasonably good linear fit with a high correlation coefficient of 0.99 or 0.98 for the thermal diffusivities of these composites vs. the volume fraction of fibers, which is closely associated with the highly ordered arrangement of continuous MPGFs in the 1-D composite block. The nearly straight-line relationship shows that the measured values of the thermal diffusivity of the composites based on continuous MPGFs is directly proportional to the fiber concentration. Based on the processing method reported in references [14,17], as the function value of x in the fit equation was extrapolated to 100, i.e. supposing a theoretical fiber volume fraction to approach 100%, the calculated data (y value) for a 100% concentration approximately corresponds to the thermal diffusivity values of the MPGFs themselves. Consequently, the room-temperature axial thermal diffusivity values of 2900 °C graphitized MPGFs with diameters of 50~55 and 10~15 μm are

about 528 and 184 mm²/s, respectively. If the bulk density and specific heat capacity of these 2900 °C graphitized MPGFs are defined as 2.2 g/cm³ and 0.71 J/g K, their corresponding room-temperature axial thermal conductivities are calculated to be 825 and 287 W/m K, respectively. It has never previously been demonstrated that there is such a great differential between the axial thermal conductivities of large and small diameter MPGFs graphitized at the same temperature. These results are based on the very large differences in the thermal conductivities of MPGFs and ABS resin (a thermal insulation plastic, its λ is about only 0.2 W/m K). Nevertheless, there is an unknown interfacial thermal resistance differential between the small and large MPGFs and the ABS resin. The interfacial area of small MPGFs is obviously larger than that of large MPGFs at the same volume fraction. (The approximate number of MPGFs in the transverse section is inversely proportional to the square of diameter). The heat dissipation or percolation from the small MPGFs to ABS resin cannot be ignored [32,33] and this may result in the effective decrease of the axial thermal conductivity of these fibers. However, the large MPGFs with open-wedge carbon layers allow much easier heat transportation in the fibers' radial direction to the ABS resin in comparison with the small MPGFs. Therefore, it is necessary to take into account the balance of both of these effects. According to the result reported in reference [34], the axial thermal conductivities of mesophase pitch-based carbon fibers (P-25 and K-1100) can be accurately determined from axially aligned unidirectional epoxy composites with high volume fraction of fibers through laser flash measurements.

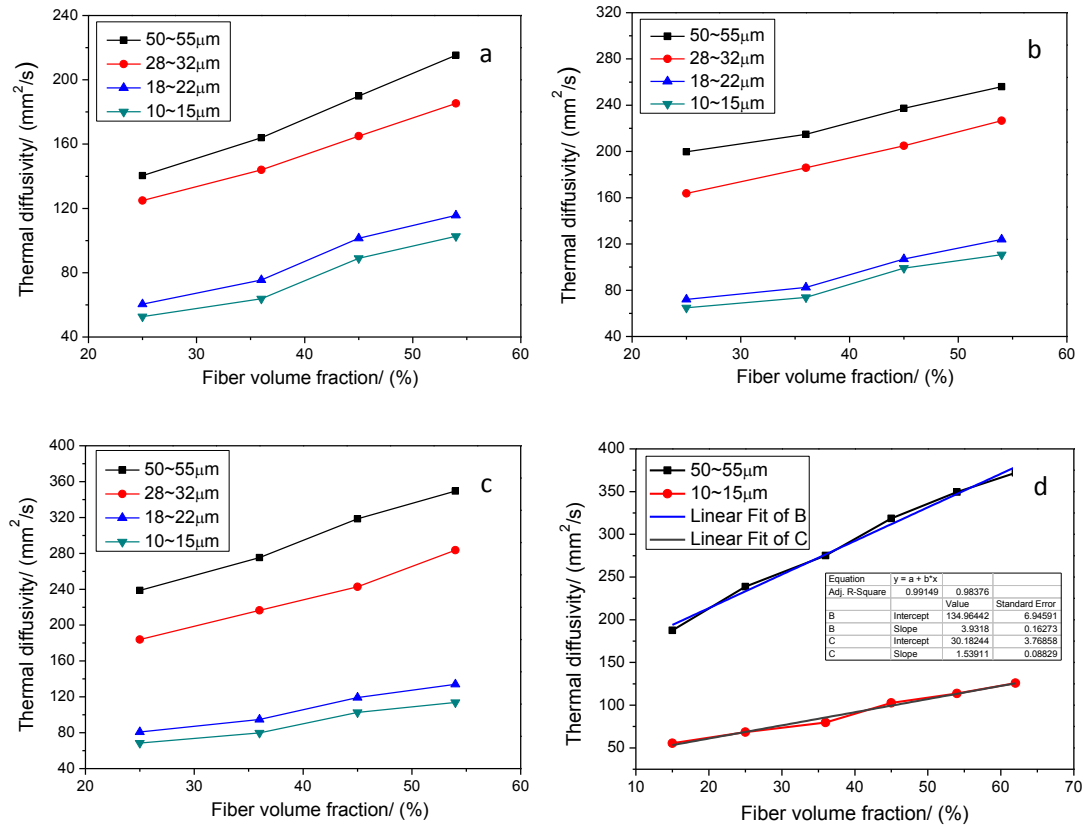


Fig. 11 Changes in thermal diffusivities of the 1-D MPGF/ABS resin composites along the fiber longitudinal direction as these vary with the volume fractions, diameters and graphitization temperatures of the fibers (a) 2500, (b) 2700 and (c) 2900 °C, (d) linear fit curves.

According to Lavin's thermal-electrical correlation ($\lambda = 440,000 / (100\rho + 258) - 295$) [35], the room-temperature axial thermal conductivities of these large and small diameter MPGFs treated at 2900 °C, based on their corresponding axial electrical resistivities (1.30~1.40 $\mu\Omega$ m), are about 810~840 W/m K [36], which is not consistent with the above result (for the small fibers). This indicates that it may be not appropriate to use Lavin's correlation to estimate the axial thermal conductivity of these MPGFs with various diameters and transverse textures as shown in Fig. 2. It is now well accepted that the thermal transportation mechanism of carbon or graphite

materials with high graphitization degree is mainly dominated by phonons, and electrons and/or holes account for the electrical conduction. Thermal transport by phonons is limited by two principal mechanisms: scattering at crystallite grain boundaries, and scattering at point defects within the layer planes [11]. Therefore, the thermal conduction with MPGFs and their directional composites is mostly governed by the phonon mean free path (closely associated with the planar crystallite size), the preferred orientation and the structural continuity of graphite crystals or layers within the fibers. It is therefore reasonable that the large MPGFs which possess large crystallite size (listed in Table 1) and greater crystal orientation (shown in Fig. 2) should have a high axial thermal conductivity.

Fig. 12 shows that the transverse thermal diffusivities of the 2-D MPGF/ABS resin composites also increase with the volume fractions, diameters and graphitization temperatures of fibers. Unexpectedly, the thermal diffusivities of the 2-D MPGF/ABS resin composites are obviously higher than those of the 1-D MPGF/ABS resin composites made with the same volume fraction of large diameter fibers of 50~55 μm as shown in Fig. 13(a). A possible explanation is that the open-wedged carbon layers within the large MPGFs are beneficial for heat transportation along the radial direction of fiber and the possibility of contact and thermal percolation between these carbon fibers may play an important role [32-34]. For MPGF/ABS resin composites made with small diameter fibers of 10~15 μm , the thermal diffusivities of the 2-D MPGF/ABS resin composites are higher than those of the 1-D MPGF/ABS resin composites only in the case of composites with fiber volume fractions above 45% as shown in Fig. 13(b) and this further indicates that a possible contact effect and thermal percolation role cannot be ignored. The mechanisms of thermal conduction and interfacial thermal resistance within such 2-D MPGF/ABS resin composites are

still under study.

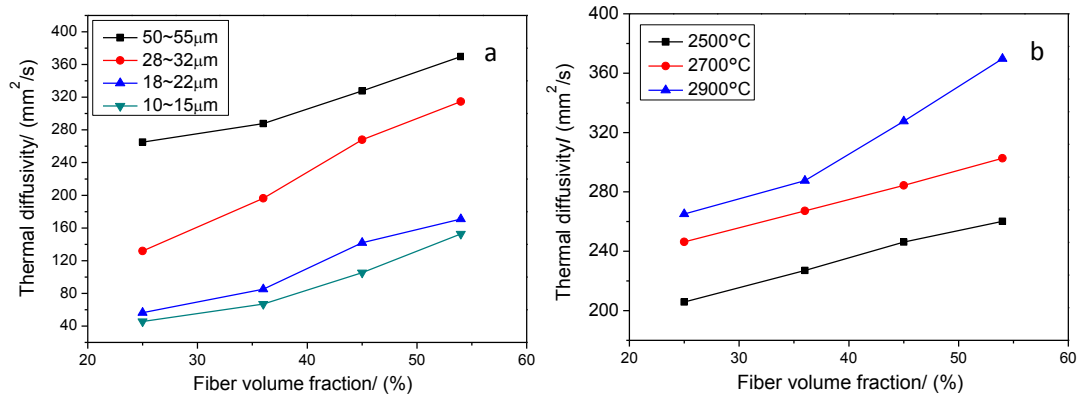


Fig. 12 The transverse thermal diffusivities of 2-D MPPG/ABS resin composites as they vary with the volume fractions, diameters and graphitization temperatures of the fibers (a) with various diameters graphitized at 2900 °C and (b) with a diameter of 50~55 μm graphitized at various temperatures.

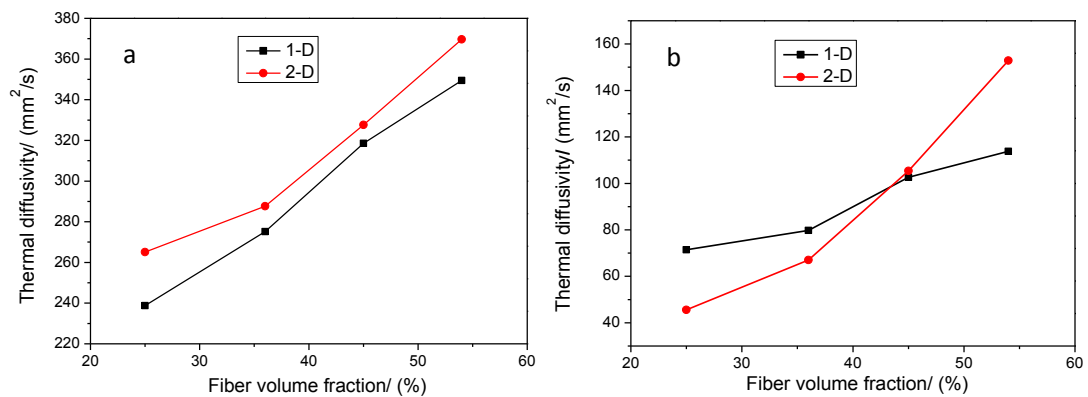


Fig. 13 The thermal diffusivities of 1-D and 2-D MPPG/ABS resin composites as they vary with the volume fractions of 2900 °C graphitized fibers having diameters of (a) 50~55 and (b) 10~15 μm.

Fig. 14 shows the bulk densities, calculated specific heat capacities, and the calculated thermal conductivities of the 1-D and 2-D MPPG/ABS resin composites

made with various volume fractions of 2900 °C graphitized fibers with a diameter of 50~55 μm. It can be seen from Fig. 14(a) that the bulk densities and calculated specific heat capacities of the 1-D and 2-D MPGF/ABS resin composites increase and decrease with the fiber volume fractions, respectively. The higher the volume fraction, the closer the calculated specific heat capacity of the composites approaches to the theoretical value (0.71 J/g K) of graphite. As can be seen from the graph shown in Fig. 14(b), the calculated thermal conductivities of the 1-D and 2-D MPGF/ABS resin composites along fiber longitudinal direction significantly increase with the fiber volume fractions. It is clear that the thermal properties of composites depend strongly on the reinforcement contents. The 1-D MPGF/ABS resin composite made with the 2900 °C graphitized fibers with a diameter of 50~55 μm at a volume fraction of 62% possesses a high calculated thermal conductivity of 518 W/m K along fiber longitudinal direction at room temperature, although this is slightly lower than the results (540~660 W/m K) reported elsewhere [2,3,15]. There is a reasonably good linear fit with a high correlation coefficient of 0.99 for the thermal conductivity of the 1-D composites vs. volume fraction of MPGFs. As the theoretical volume fraction of fibers is extrapolated to 100% (without consideration of the geometric packing limit on the actual volume fraction of fibers in composites), the room-temperature axial thermal conductivity value of 2900 °C graphitized MPGFs with a diameter of 50~55 μm is about 740 W/m K, which is little lower than the fitting result of Fig. 11(d) (825 W/m K). This discrepancy appears to be due to differences in the specific heat capacity of MPGF/ABS resin composites calculated according to the mixture rule as shown in Fig. 14(a), which varies from 1.14 to 0.85 J/g K as the fiber volume fraction varies from 15% to 62%. In addition, the radial crack texture of carbon fibers with a large diameter may be helpful for heat dissipation or percolation from the carbon

fibers to ABS resin, such heat scattering thus leading to the decrease of the thermal conductivity of composites. As a comparison, in terms of the rule of mixture for the thermal conductivity of fiber-reinforced 1-D composites [19,34,37], according to the measured values ($V_f = 62\%$, $V_m = 38\%$, $\lambda_c = 518 \text{ W/m K}$, $\lambda_m = 0.2 \text{ W/m K}$) and estimation of λ (without consideration of the interfacial thermal interaction), the large MPGFs would have a mean axial thermal conductivity of 835 W/m K , which is very close to the fitting result of 825 W/m K and higher than the fitting result of 740 W/m K . Therefore, it is more feasible and reasonable to evaluate the axial thermal conductivity of MPGFs by using the longitudinal thermal diffusivities of the 1-D MPGF/ABS resin composites.

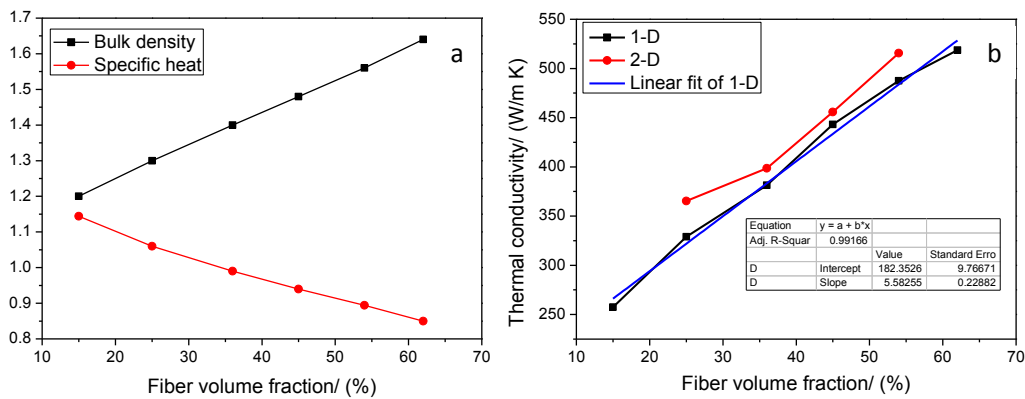


Fig. 14 The (a) bulk densities and calculated specific heat capacities, and (b) calculated thermal conductivities of the 1-D and 2-D MPGF/ABS resin composites varying with the volume fractions of $2900 \text{ }^\circ\text{C}$ graphitized fibers with a diameter of $50\sim 55 \text{ }\mu\text{m}$.

Table 2 lists the thermal diffusivities and calculated thermal conductivities of the 1-D and 2-D MPGF/ABS resin composites made with $2900 \text{ }^\circ\text{C}$ graphitized fibers with a diameter of $50\sim 55 \text{ }\mu\text{m}$ at high fiber volume fractions determined in different

directions. The 1-D composite made with the 2900 °C graphitized fibers with a diameter of 50~55 μm at a volume fraction of 62% possesses a high thermal diffusivity of 372 mm²/s and a correspondingly high calculated thermal conductivity of 518 W/m K along the fiber longitudinal direction at room temperature. This is higher than the corresponding values for copper (~117 mm²/s and 400 W/m K). The bulk density of the composite is about 1.64 g/cm³, less than one fifth of that of copper (8.9 g/cm³). This means that the specific thermal conductivity, i.e., thermal conductivity divided by the density, of the composite block is seven times higher than that of copper. However, in another direction, i.e. perpendicular to the hot-pressed surface of the composite block, the thermal diffusivity and calculated thermal conductivity are found to be as low as 1.3 mm²/s and 1.8 W/m K, i.e. only slightly higher than the values for ABS resin (0.14 mm²/s and 0.2 W/m K). These obvious differences in thermal transport behavior in the two directions result from the structural anisotropy as evidenced in Fig. 5 and Fig. 9. It is well known that the thermal diffusivity and thermal conductivity in the transverse direction of MPGFs is at least an order of magnitude lower than those in the axial direction, similar to that of 'c' and 'a' axes of natural graphite [12,38]. Moreover, the ABS resin is a thermally insulating material with potentially high interfacial thermal resistance. Therefore, the composite blocks are still thermally insulating in the direction perpendicular to the hot-pressed surface. It is interesting to note that the thermal diffusivity and calculated thermal conductivity, in the direction perpendicular to the transverse section of the 2-D MPGF/ABS resin composites made with 2900 °C graphitized fibers with a diameter of 50~55 μm at a volume fraction of 54% in two directions, are nevertheless found to be very high (496~515 W/m K). This could therefore offer high thermal conductivity in two dimensions or in-plane to satisfy specific thermal management

demands rather than being limited to only one direction. The thermal diffusivity and calculated thermal conductivity of the 2-D MPGF/ABS resin composites in the direction perpendicular to the hot-pressed surface of the composite block are still low, but larger than those of the 1-D composites loaded with the same volume fraction of fibers. The latter observation indicates that the contact effect is in operation for heat dissipation between MPGFs. The probability of contacting each other for MPGFs arranged alternately in the 2-D composites, as shown in Fig. 4, is relatively greater than that in the 1-D composites, and this is of benefit for heat transport within two in-plane dimensions and may explain the higher thermal diffusivity of the 2-D composites compared with that of the 1-D composites, as shown in Fig. 13(b).

Table 2 The thermal diffusivities and calculated thermal conductivities of the 1-D and 2-D MPGF/ABS resin composites made with 2900 °C graphitized fibers with a diameter of 50~55 μm at room temperature.

Architecture	Vol. (%)	ρ (g/cm ³)	α (mm ² /s)	λ (W/m K)	Testing direction
1-D	54	1.56	349.5	487.4	//
			1.2	1.67	\perp
1-D	62	1.64	372.1	518.7	//
			1.3	1.8	\perp
2-D	54	1.56	369.7	515.6	—
			356.1	496.6	—
			1.7	2.37	\perp

// - parallel to fiber longitudinal direction, \perp - perpendicular to hot-pressed surface,

— perpendicular to transverse section.

3.5 Electrical properties of the MPGF/ABS resin composites

The influence of the volume fraction of carbon fibers on the room-temperature electrical resistivity of the 1-D MPGF/ABS resin composites along the fiber longitudinal direction is shown in Fig. 15. It can be seen from the graph in Fig. 15 that the electrical resistivity of the 1-D MPGF/ABS resin composite blocks obviously decreases with the increase of fiber volume fraction. ABS resin block is a typical electrical insulator and its room-temperature electrical resistivity is reported to be as high as $10^{13} \Omega \text{ m}$ [39]. The electrical resistivity of the 1-D composite blocks retain high electrical resistivities similar to that of ABS resin until the fiber volume fraction approaches to 20%. Thereafter, as the fiber volume fraction increases to 62%, the electrical resistivity of the 1-D composite blocks sharply decreases to about $7 \Omega \text{ m}$ and the MPGF/ABS resin composites exhibit electrically conductive properties in the fiber longitudinal direction similar to that of a semi-conductive plastic.

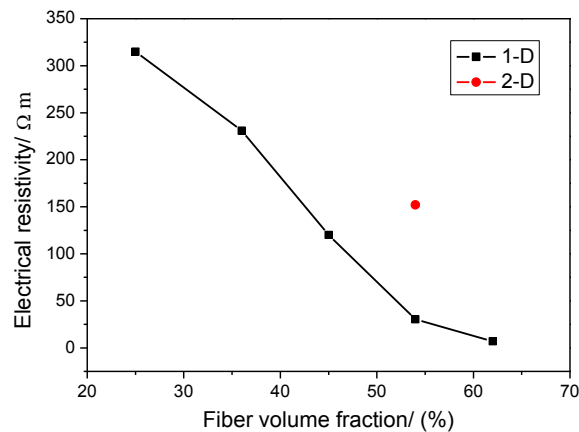


Fig. 15 The electrical resistivity of the 1-D MPGF/ABS resin composites as it varies with volume fraction of 2500 °C graphitized fibers with a diameter of 50~55 μm .

The electrical resistivity of the 2-D composite blocks perpendicular to its transverse section is obviously higher than that of the 1-D composites at the same fiber volume

fraction of 54%. The electrical resistivities of the composite blocks perpendicular to the hot-pressed surface are very high ($10^8 \sim 10^9 \Omega \text{ m}$), similar to that of ABS resin, and this is the result of relatively low electrical conductivity in the radial direction of the carbon fiber and the very limited contact between the MPGFs (as already mentioned in the context of thermal conductivity). Such MPGF/ABS resin composites with high thermal conductivity in one direction but an electrically insulating property in another direction are very suitable for heat dissipation in high power electronic packaging applications [14].

3.6 Mechanical properties of the MPGF/ABS resin composites

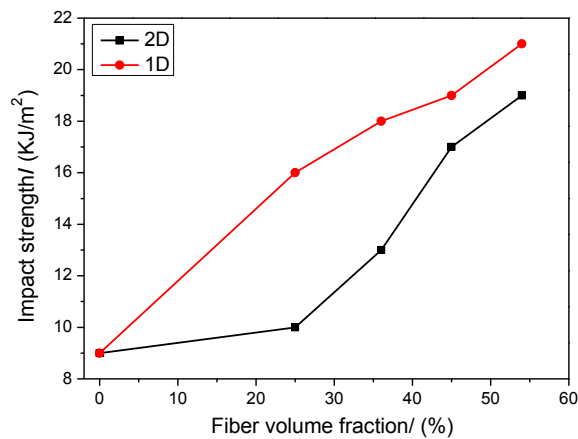


Fig. 16 The impact strength of the 1-D and 2-D MPGF/ABS resin composites versus volume fraction of 2500 °C graphitized fibers with a diameter of 50~55 μm .

The room-temperature impact strengths perpendicular to the longitudinal direction of graphite fibers for the 1-D and 2-D MPGF/ABS resin composite blocks are shown in Fig. 16. As can be seen from the graph in Fig. 16, the impact strengths of the 1-D and 2-D MPGF/ABS resin composite blocks obviously increase with fiber volume fraction. The impact strength of the ABS resin block is about 9 KJ/m^2 but this significantly increases to about 20 KJ/m^2 as the volume fraction of reinforcing fibers

risers to 54%. The impact strength of the 1-D composite blocks is higher than that of the 2-D composites at the same volume fraction of fibers. It is obvious that loading of continuous MPGFs into ABS resin can effectively improve the resin's mechanical property.

4. Conclusions

1-D and 2-D MPGF/ABS resin composite blocks were easily fabricated by a simple hot-pressing method. Their XRD, PLM and SEM analyses show that the MPGFs are in a well ordered arrangement in the composites. The prepared composite blocks possess a typical structural anisotropy, which results from the anisotropic structure of the MPGFs themselves and the directional arrangement of the MPGFs in the composites, and thus leads to obvious differences in the thermal and electrical conduction behaviors of the composite within two orthogonal planes. The thermal diffusivity and thermal conductivity of the composites along the longitudinal direction of graphite fiber obviously increase with the volume fraction, the diameter and the graphitization temperature of the fibers. The 1-D composite made with the 2900 °C graphitized fibers with a diameter of 50~55 μm at a volume fraction of 62% possesses a low density of 1.64 g/cm³ and shows a high thermal diffusivity of 372 mm²/s and a high calculated thermal conductivity of 518 W/m K along fiber longitudinal direction at room temperature. These values are significantly higher than those of copper. The 2-D composites made with such graphite fibers at high volume fractions also exhibit relatively high thermal diffusivity and thermal conductivity properties in two dimensions. Such composite blocks exhibit thermal insulation and electric insulation and an obviously improved mechanical behavior in the direction perpendicular to the hot-pressed surface. The 1-D and 2-D MPGF/ABS resin composite blocks with high

thermal conductivity in one direction and two-directions, respectively, can be expected to offer strong applicability thermal management roles.

The room-temperature axial thermal conductivity of 2900 °C graphitized MPGFs with a diameter of 50~55 μm is estimated to be 825 W/m K through extrapolation by using the longitudinal thermal diffusivities (as opposed to thermal conductivities) of the 1-D MPGF/ABS resin composites, which is in good agreement with the thermal conductivity values of 840 and 835 W/m K calculated by Lavin's thermal-electrical correlation and the rule of mixture, respectively. However, the estimated axial thermal conductivity of the small fibers with a diameter of 10~15 μm is less than 300 W/m K (without consideration of interfacial thermal dissipation), which indicates that it may be not appropriate to estimate the thermal conductivity of these MPGFs by Lavin's correlation owing to the obvious differences in the transverse texture, crystal size and orientation of the fibers. The crystal size and crystal orientation of the MPGFs are strongly influenced by fiber diameter and graphitization temperature and they dominate their thermal conduction property, which beyond doubt controls the thermal conductivities of the resultant composites. The anisotropic thermal transportation characteristic of the MPGFs is clearly manifested in the low-dimensional (1-D and 2-D) polymer matrix composites.

Acknowledgements

This work was sponsored by the National Natural Science Foundation of China (grant No. 91016003 & 51372177), and Hubei Provincial Department of Education Science Research Project (Q20141104). The authors sincerely thank Dr. Hongda Du for thermal conductivity measurements.

References

- [1] Jiang GS. Introduction to thermal management in microelectronics packaging. In: Jiang GS, Diao LY, Kuang K, editors. *Advanced thermal management materials*, New York: Springer Science + Business Media; 2013, P. 1–10.
- [2] Zweben C. Advances in composite materials for thermal management in electronic packaging. *JOM* 1998;50(6):47–51.
- [3] Chung DDL, Zweben C. Composites for electronic packaging and thermal management. In: Kelly A, Zweben C, editors. *Comprehensive composite materials*, vol 6, Oxford: Pergamon Press; 2000, P. 701–25.
- [4] Zweben C. High-performance thermal management materials. *Adv Packaging* 2006;15(2):1–5.
- [5] Edie DD, Robinson KE, Fleurot O, Jones SP, Fain CC. High thermal conductivity ribbon fibers from naphthalene-based mesophase. *Carbon* 1994;32(6):1045–54.
- [6] Minus ML, Kumar S. The processing, properties, and structure of carbon fibers. *J Microsc* 2005;57(2):52–8.
- [7] Emmerich FG. Young's modulus, thermal conductivity, electrical resistivity and coefficient of thermal expansion of mesophase pitch-based carbon fibers. *Carbon* 2014;68:274–93.
- [8] Sheehan JE, Buesking KW, Sullivan BJ. Carbon-carbon composites. *Annu Rev Mater Sci* 1994;24:19–44.
- [9] Lackey WJ. Carbon-carbon composites. In: Buschow KHJ, Cahn RW, Flemings MC, Iischer B, Kramer EJ, Mahajan S, Veysiere P, editors. *Encyclopedia of materials: science and technology*, London: Pergamon Pr Publisher; 2001, P. 952–67.
- [10] Manocha LM. Thermophysical properties of densified pitch based carbon/carbon materials-I. Unidirectional composites. *Carbon* 2006;44(3):480–7.

- [11] Adams PM, Katzman HA, Rellick GS, Stupian GW. Characterization of high thermal conductivity carbon fibers and a self-reinforced graphite panel. *Carbon* 1998;36(3):233–45.
- [12] Yuan GM, Li XK, Dong ZJ, Xiong XQ, Rand B, Cui ZW, et al. Pitch-based ribbon-shaped carbon-fiber-reinforced one-dimensional carbon/carbon composites with ultrahigh thermal conductivity. *Carbon* 2014;68:413–25.
- [13] Bertram A, Beasley K, Delatorre W. An overview of navy composite developments for thermal management. *Nav Eng J* 1992:276–85.
- [14] Chen YM, Jyh-Ming T. Ultra high thermal conductivity polymer composites. *Carbon* 2002;40(3):359–62.
- [15] Thomas F, Fleming, Riley, William C. Applications for ultra-high thermal conductivity graphite fibers. *High Heat Flux Eng II* 1997:136–47.
- [16] Yuan GM, Li XK, Dong ZJ, Westwood A, Rand B, Cui ZW, et al. The structure and properties of ribbon-shaped carbon fibers with high orientation. *Carbon* 2014;68:426–39.
- [17] Nysten B, Issi JP. Composites based on thermally hyperconductive carbon fibres. *Composites* 1990;21(4):339–43.
- [18] Tsukuda R, Sumimoto S, Ozawa T. Thermal conductivity and heat capacity of ABS resin composites. *J Appl Polym Sci* 1997;63(10):1279–86.
- [19] Korab J, Stefanik P, Kavecky S, Sebo P, Korb G. Thermal conductivity of unidirectional copper matrix carbon fibre composites. *Compos Part A–Appl S* 2002;33(4):577–81.
- [20] Jeon YP, Cooper RA, Morales M, Ogale AA. Carbon fibers. In: Somiya S, editor. *Handbook of advanced ceramics-materials, applications, processing, and properties*, 2nd ed. Academic Press; 2013, P. 143–54.

- [21] Blanco C, Appleyard SP, Rand B. Study of carbon fibres and carbon–carbon composites by scanning thermal microscopy. *J Microsc* 2002;205(1):21–32.
- [22] Mochida I, Yoon SH, Takano N, Fortin F, Korai Y, Yokogawa K. Microstructure of mesophase pitch-based carbon fiber and its control. *Carbon* 1996;34(8):941–56.
- [23] Yoon SH, Takano N, Korai Y, Mochida I. Crack formation in mesophase pitch-based carbon fibres: Part I some influential factors for crack formation. *J Mater Sci* 1997;32(10):2753–8.
- [24] Lu SL, Blanco C, Rand B. Large diameter carbon fibres from mesophase pitch. *Carbon* 2002;40(12):2109–16.
- [25] Takahashi H, Kuroda H, Akamatu H. Correlation between stacking order and crystallite dimensions in carbons. *Carbon* 1965;2(4):432–3.
- [26] Maire J, Mering J. Graphitization of soft carbons. In: Walker PL, editor, *Chemistry and physics of carbon*, New York: Marcel Dekker; 1970, P. 125–90.
- [27] Edie DD. The effect of processing on the structure and properties of carbon fibers. *Carbon* 1998;36(4):345–62.
- [28] Yuan GM, Li XK, Dong ZJ, Westwood A, Cui ZW, Cong Y, et al. Graphite blocks with preferred orientation and high thermal conductivity. *Carbon* 2012;50(1):175–82.
- [29] Hishiyama Y, Nakamura M. X-ray diffraction in oriented carbon films with turbostratic structure. *Carbon* 1995;33(10):1399–403.
- [30] Chen GH, Wang HQ, Zhao WF. Fabrication of highly ordered polymer/graphite flake composite with eminent anisotropic electrical property. *Poly Adv Technol* 2008;19(8):1113–7.
- [31] Chung DDL. Materials for thermal conduction. *Appl Therm Eng* 2001;21(16):1593–605.
- [32] Kumar S, Alam MA, Murthy JY. Effect of percolation on thermal transport in

- nanotube composites. *Appl Phys Lett* 2007;90:104105 1–3.
- [33] Zheng RT, Gao JW, Wang JJ, Feng SP, Ohtani H, Wang JB, et al. Thermal percolation in stable graphite suspensions. *Nano Lett* 2012;12(1):188–92.
- [34] Alway-Cooper RM, Theodore M, Anderson DP, Ogale AA. Transient heat flow in unidirectional fiber–polymer composites during laser flash analysis: Experimental measurements and finite element modeling. *J Compos Mater* 2012;47(19):2399–411.
- [35] Lavin JG, Boyington DR, Lahijani J, Nystem B, Issi JP. The correlation of thermal conductivity with electrical resistivity in mesophase pitch-based carbon fiber. *Carbon* 1993;31(6):1001–2.
- [36] Yuan GM, L XK, Zhou J, Dong ZJ, Cui ZW, Cong Y, et al. Controlled preparation of mesophase pitch-based highly oriented carbon fibers with different shapes. Extended abstracts, an International Conference on Carbon 2012. Krakow (Poland): Polish Carbon Society, 2012; P. 1–4.
- [37] Hasselman DPH, Donaldson KY, Thomas JR. Effective thermal-conductivity of uniaxial composite with cylindrically orthotropic carbon-fibers and interfacial thermal barrier. *J Compos Mater* 1993;27(6):637–44.
- [38] Norley J. The role of natural graphite in electronics cooling. *Electronics Cooling* 2001;7:50–1.
- [39] Liang XY, Ling LC, Lu CX, Liu L. Resistivity of carbon fibers/ABS resin composites. *Matter Lett* 2000;43(3):144–7.